



ISSN: 0975-833X

Available online at <http://www.journalcra.com>

INTERNATIONAL JOURNAL  
OF CURRENT RESEARCH

International Journal of Current Research

Vol. 10, Issue, 12, pp.76406-76412, December, 2018

DOI: <https://doi.org/10.24941/ijcr.33756.12.2018>

## RESEARCH ARTICLE

### PKM2 IS A TARGET OF HUHS1015 FOR INDUCING COLONIC CANCER CELL DEATH

\*Tomoyuki Nishizaki

Innovative Bioinformation Research Organization, Kobe, Japan

#### ARTICLE INFO

##### Article History:

Received 09<sup>th</sup> September, 2018

Received in revised form

10<sup>th</sup> October, 2018

Accepted 30<sup>th</sup> November, 2018

Published online 31<sup>st</sup> December, 2018

##### Key Words:

HUHS1015, PKM2,

Autophagic degradation,

Colonic cancer cell, Cell death.

#### ABSTRACT

The newly synthesized naftopidil analog HUHS1015 has been developed as an anticancer drug. The present study aimed at understanding the mechanism underlying HUHS1015-induced cell death in CW2 and Caco-2 human colonic cancer cells. HUHS1015 reduced cell viability in CW2 and Caco-2 cells in a concentration (10-100  $\mu$ M)-dependent manner. HUHS1015 decreased pyruvate kinase M2 (PKM2) protein, and the effect was inhibited by the autophagy inhibitor 3-methyladenine. PKM2 deficiency activated caspase-3, -4, -8, and -9 in Caco-2 cells, although such effect was not obtained with CW2 cells. Moreover, PKM2 deficiency induced early apoptosis and late apoptosis/secondary necrosis in CW2 cells and primary necrosis, early apoptosis, and late apoptosis/secondary necrosis in Caco-2 cells. The results of the present study show that HUHS1015 decreases PKM2 protein due to autophagic degradation, to initiate cell death such as necrosis and caspase-dependent and -independent apoptosis in CW2 and Caco-2 cells.

**Copyright** © 2018, Tomoyuki Nishizaki. This is an open access article distributed under the Creative Commons Attribution License, which permits unrestricted use, distribution, and reproduction in any medium, provided the original work is properly cited.

**Citation:** Tomoyuki Nishizaki. 2018. "Pkm2 is a target of huhs1015 for inducing colonic cancer cell death.", *International Journal of Current Research*, 10, (12), 76406-76412.

## INTRODUCTION

The naftopidil analogue 1-[2-(2-methoxyphenylamino)ethylamino]-3-(naphthalene-1-yloxy)propan-2-ol (HUHS1015) has been developed as an anticancer drug. HUHS1015 induces cell death in MSTO-211H, NCI-H28, NCI-H2052, and NCI-H2452 human malignant mesothelioma cells; A549, SBC-3, and Lu-65 human lung cancer cells; HepG2 and HuH-7 human hepatoma cells; MKN28 and MKN45 human gastric cancer cells; CW2 and Caco-2 human colonic cancer cells; 253J, 5637, KK-47, TCCSUP, T24, and UM-UC-3 human bladder cancer cells; DU145, LNCaP, and PC-3 human prostate cancer cells; and ACHN, RCC4-VHL, and 786-O human renal cancer cells through diverse signal transduction pathways (Kanno *et al.*, 2013; Nishizaki *et al.*, 2014). For colonic cancer cells, HUHS1015 induces necrosis by lowering the intracellular ATP levels in association with mitochondrial damage as well as caspase-dependent apoptosis (Kaku *et al.* 2016). Intriguingly, HUHS1015 decreases X-linked inhibitor of apoptosis protein (XIAP) due to autophagic degradation, which triggers caspase-3 activation followed by apoptotic cell death in CW2 cells (Tsuchiya *et al.*, 2015). The present study was conducted to gain further insight into the mechanism underlying HUHS1015-induced cell death in colonic cancer cells. The results show that HUHS1015 promotes autophagic degradation of pyruvate kinase M2 (PKM2) protein, causing cell death in CW2 and Caco-2 cells.

\*Corresponding author: Tomoyuki Nishizaki,

Innovative Bioinformation Research Organization, Kobe, Japan.

## MATERIALS AND METHODS

**Cell culture:** CW2 and Caco-2 cell lines were obtained from RIKEN cell bank (Ibaraki, Japan). Cells were cultured in a Dulbecco's modified Eagle's medium supplemented with 10% heat-inactivated fetal bovine serum, penicillin (final concentration, 100 U/ml), and streptomycin (final concentration, 0.1 mg/ml), in a humidified atmosphere of 5% CO<sub>2</sub> and 95% air at 37 °C.

**Cell viability:** Cell viability was evaluated by the 3-(4,5-dimethyl-2-thiazolyl)-2,5-diphenyl-2H-tetrazolium bromide (MTT) method as previously described (Saitoh *et al.*, 2011).

**Western blotting:** After treatment, cells were lysed and the lysates were loaded onto sodium dodecyl sulfate-polyacrylamide gel electrophoresis (SDS-PAGE) and transferred to polyvinylidene difluoride membrane. The blotting membrane was reacted with antibodies against PKM2 (Cosmo Bio, Tokyo, Japan) and  $\beta$ -actin (Cell Signaling, Beverly, MA, USA), followed by a horseradish peroxidase (HRP)-conjugated anti-mouse IgG antibody. Immunoreactivity was detected with an ECL kit (Invitrogen, Carlsbad, CA, USA) and visualized using a chemiluminescence detection system (GE Healthcare, Piscataway, NJ, USA). Protein concentrations for each sample were determined with a BCA protein assay kit (Thermo Fisher Scientific, Rockford, IL, USA).

**Real-time reverse transcription-polymerase chain reaction (RT-PCR):** Total RNAs from cells were purified by an acid/guanidine/thiocyanate/chloroform extraction method using the Sepasol-RNA I Super kit (Nacalai, Kyoto, Japan). After purification, total RNAs were treated with RNase-free Dnase I (2 units) at 37 °C for 30 min to remove genomic DNAs, and 10 mg of RNAs was resuspended in water. Random primers, dNTP, 10× RT buffer, and Multiscribe Reverse Transcriptase were then added to the RNA solutions and incubated at 25 °C for 10 min, followed by 37 °C for 120 min to synthesize the first-strand cDNA. Real-time RT-PCR was performed using a SYBR Green Realtime PCR Master Mix (Takara Bio) and the Applied Biosystems 7900 real-time PCR detection system (ABI, Foster City, CA, USA). Thermal cycling conditions were as follows: first step, 94 °C for 4 min; the ensuing 40 cycles, 94 °C for 1 s, 65 °C for 15 s, and 72 °C for 30 s. The primers used were as follows: (Forward) ATTGCCCGAGAGGCAGAGGC and (Reverse) ATCAAGGTACAGGCACTACACGCAT for PKM2; and (Forward) GACTTCAA CAGCGACACCCACTCC and (Reverse) AG GTCCACCACCCTGTTGCTGTAG for glyceraldehyde 3-phosphate dehydrogenase (GAPDH). The quantity of the PKM2 mRNA was normalized by that of the GAPDH mRNA.

**Knockdown of PKM2 protein:** The siRNA to silence the PKM2-targeted gene was obtained from Santa Cruz Biotechnology (Santa Cruz, CA, USA) and the negative control (NC) siRNA from Ambion (Carlsbad, CA, USA). siRNAs were transfected into cells using a Lipofectamine reagent (Invitrogen, Carlsbad, CA, USA), and cells were used for experiments from 48 h after transfection.

**Enzymatic caspase assay:** Caspase activity was measured using a caspase fluorometric assay kit (Ac-Asp-Glu-Val-Asp-MCA for a caspase-3 substrate peptide; Ac-Leu-Glu-Val-Asp-AFC for a caspase-4 substrate peptide; Ac-Ile-Glu-Thr-Asp-MCA for a caspase-8 substrate peptide, and Ac-Leu-Glu-His-Asp-MCA for a caspase-9 substrate peptide) by the method previously described (Yang *et al.*, 2007). Briefly, cells were harvested before and after treatment with HUHS1015, and then centrifuged at 1,200 rpm for 5 min at 4 °C. The pellet was incubated in cell lysis buffer on ice for 10 min and reacted with the fluorescently labeled tetrapeptide at 37 °C for 2 h. Fluorescence was measured at an excitation wavelength of 380 nm and an emission wavelength of 460 nm for caspase-3, -8, and -9 or an excitation wavelength of 400 nm and an emission wavelength of 505 nm for caspase-4 with a fluorometer (Fluorescence Spectrometer, F-4500, Hitachi, Japan).

**Apoptosis assay:** Cells were suspended in a binding buffer and stained with both propidium iodide (PI) and annexin V (AV)-FITC, and loaded onto a flow cytometer (FACSCalibur; Becton Dickinson, Franklin Lakes, NJ, USA) available for FL1 and FL2 bivariate analysis. Data from 20,000 cells/sample were collected, and the quadrants were set according to the population of viable unstained cells in untreated samples. CellQuest (Becton Dickinson) analysis of the data was used to calculate the percentage of the cells in the respective quadrants.

**Statistical analysis:** Statistical analysis was carried out using unpaired *t*-test and analysis of variance (ANOVA) followed by a Bonferroni correction.

## RESULTS

**HUHS1015 induces cell death in CW2 and Caco-2 cells:** HUHS1015 reduced cell viability in CW2 and Caco-2 cells in a concentration (10-100 μM)-dependent manner (Figure 1A,B). This indicates that HUHS1015 induces cell death in both the colonic cancer cell types.

**HUHS1015 decreases PKM2 protein in CW2 and Caco-2 cells due to autophagic degradation:** HUHS1015 (100 μM) decreased PKM2 protein at 10-min treatment in CW2 cells, the effect lasting at least for 60 min (Figure 2A). Likewise, HUHS1015 (100 μM) decreased PKM2 protein in a treatment time (10-60 min)-dependent manner (Figure 2B). In the real-time RT-PCR analysis, HUHS1015 (100 μM) had no effect on the PKM2 mRNA levels in CW2 cells for 30 min, although a significant decrease was found at 60-min treatment (Figure 2C). This suggests that HUHS1015-induced decrease of PKM2 protein in CW2 cells is not mainly due to downregulation of the PKM2 mRNA. In contrast, the PKM2 mRNA levels in Caco-2 cells were not affected by HUHS1015 (100 μM) throughout 10-60 min treatment (Figure 2D). This indicates that HUHS1015 decreases PKM2 protein, regardless of the mRNA transcription. HUHS1015-induced decrease of PKM2 protein in CW2 and Caco-2 cells was significantly inhibited by 3-methyladenine (3-MA), an inhibitor of autophagy (Figure 3A,B). Overall, these results indicate that HUHS1015 decreases PKM2 protein in both the cell types due to autophagic degradation.

**PKM2 is a target of HUHS1015 for inducing colonic cancer cell death:** To examine whether HUHS1015-induced decrease of PKM2 protein is a factor to induce cell death, PKM2 was knocked-down. PKM2 was successfully knocked-down by transfecting with the PKM2 siRNA in CW2 and Caco-2 cells (Figure 4A,B). In the enzymatic caspase assay, activities of caspase-3, -4, -8, and -9 in CW2 cells were not affected by knocking-down PKM2 (Figure 5A). In contrast, all the activities of caspase-3, -4, -8, and -9, especially the caspase-3 activity, in Caco-2 cells were significantly raised by knocking-down PKM2 (Figure 5B). This implies that PKM2 deficiency activates caspase-3, -4, -8, and -9 in Caco-2 cells, while PKM2 is not implicated in the caspase activation in CW2 cells. In the flow cytometry using PI and AV, the populations of PI-negative/AV-positive and PI-positive/AV-positive cells in CW2 cells, corresponding to cells undergoing early apoptosis and late apoptosis/secondary necrosis, respectively (Pietra *et al.*, 2001), significantly increased in association with significant decrease in the population of PI-negative/AV-negative cells, corresponding to alive cells, by knocking-down PKM2 (Figure 6A). The populations of PI-positive/AV-negative, PI-negative/AV-positive cells, and PI-positive/AV-positive cells in Caco-2 cells, corresponding to cells undergoing primary necrosis, early apoptosis, and late apoptosis/secondary necrosis, respectively (Pietra *et al.*, 2001), significantly increased in association with significant decrease in the population of PI-negative/AV-negative cells by knocking-down PKM2 (Figure 6B). These results indicate that PKM2 deficiency induces cell death including apoptosis and necrosis in CW2 and Caco-2 cells.

## DISCUSSION

In the present study, HUHS1015 reduced cell viability in CW2 and Caco-2 cells in a concentration (10-100 μM)-dependent manner, indicating that HUHS1015 induces cell death in both

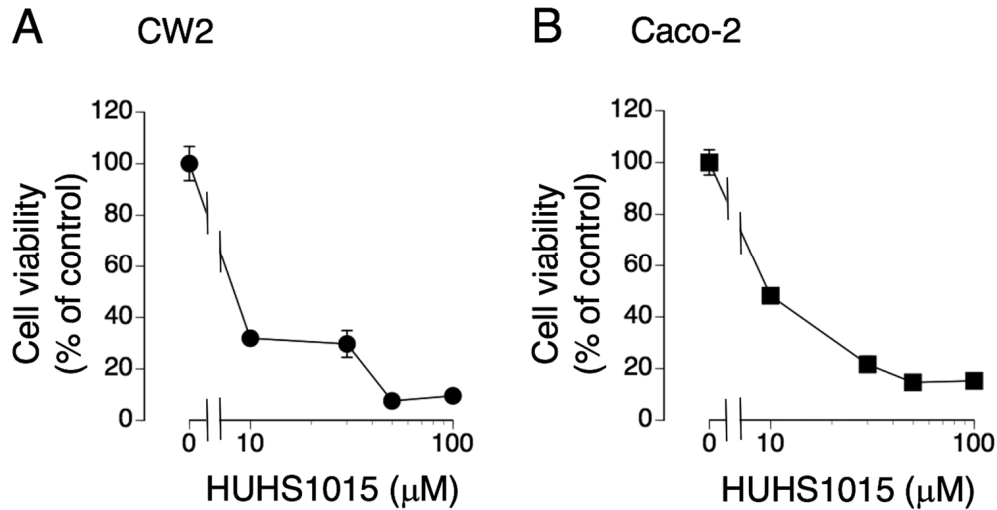


Figure 1. HUHS1015 induces cell death in CW2 (A) and Caco-2 cells (B). Cells were treated with HUHS1015 at concentrations as indicated for 24 h, and MTT assay was carried out. In the graphs, each point represents the mean ( $\pm$  SEM) percentage of control (MTT intensity of untreated control cells) (n=4 independent experiments)

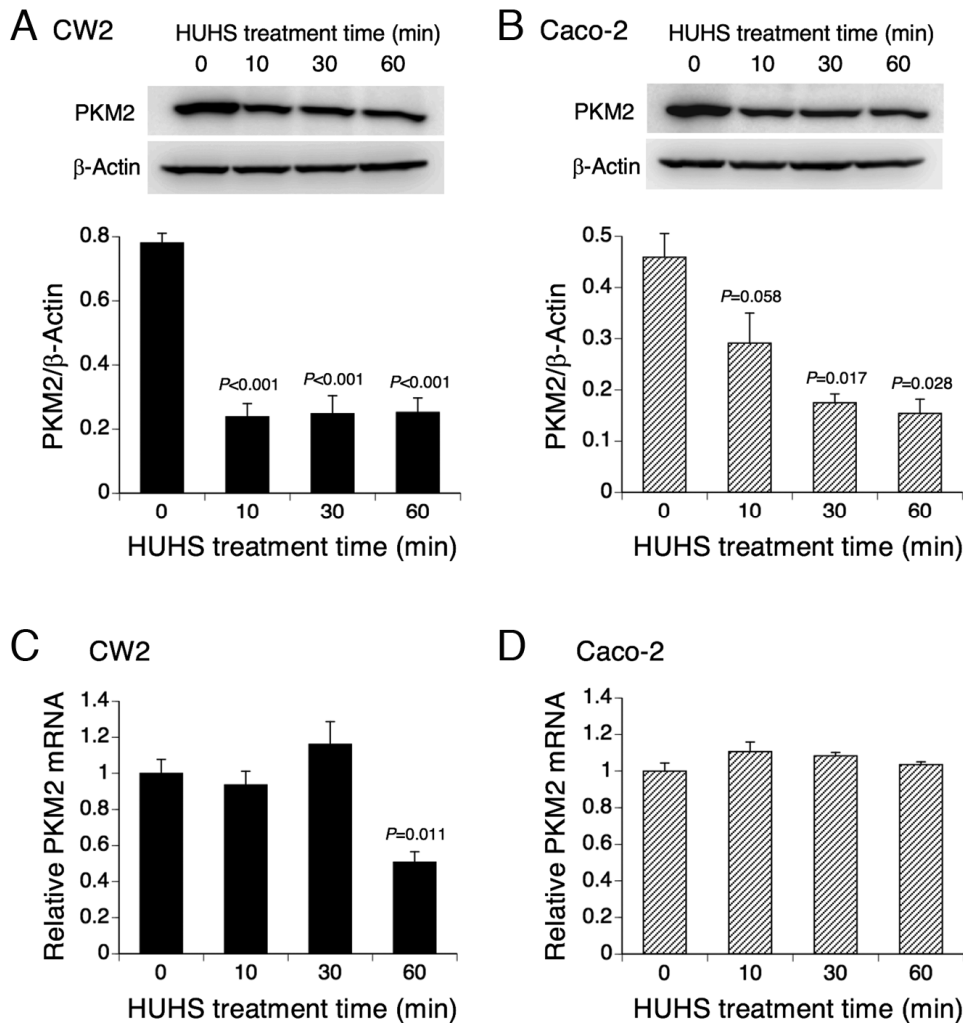
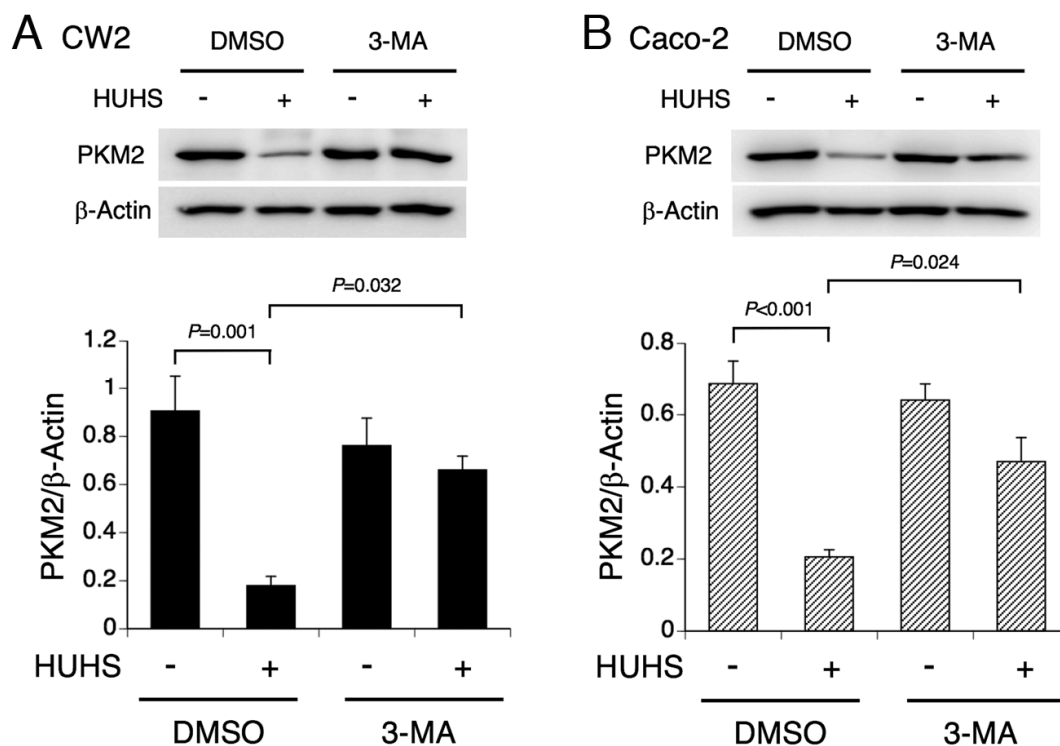
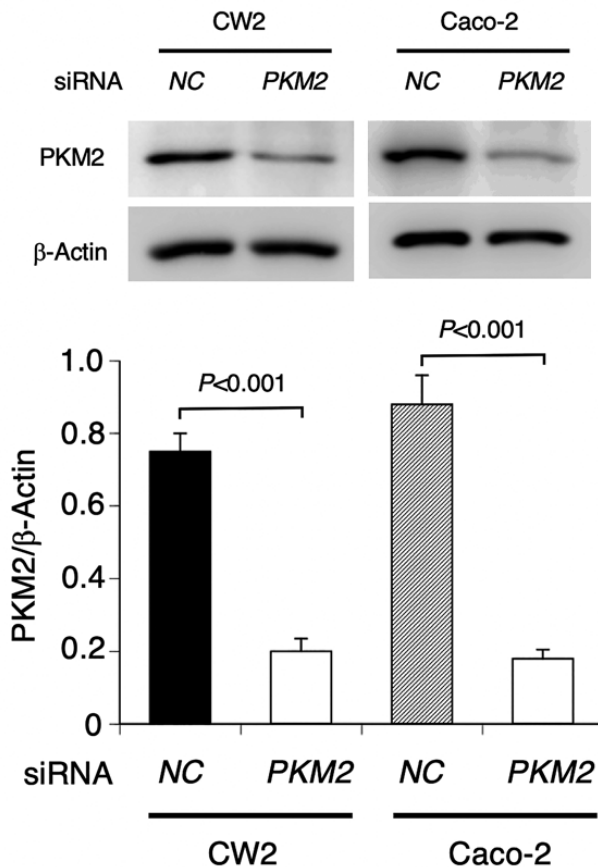


Figure 2. HUHS1015 decreases PKM2 protein. CW2 (A,C) and Caco-2 cells (B,D) were treated with HUHS1015 (100  $\mu\text{M}$ ) for periods of time as indicated, followed by Western blotting and RT-PCR. (A,B) In the graphs, each column represents the mean ( $\pm$  SEM) signal intensity for PKM2 relative to the intensity for  $\beta$ -actin (n=4 independent experiments).  $P$  values, ANOVA followed by a Bonferroni correction. (C,D) The quantity for the PKM2 mRNA was normalized by that for the GAPDH mRNA. In the graphs, each column represents the mean ( $\pm$  SEM) normalized quantity for the PKM2 mRNA relative to the quantity at 0 min (n=4 independent experiments).  $P$  value, ANOVA followed by a Bonferroni correction.



**Figure 3.** Autophagy is implicated in the HUHS1015-induced decrease of PKM2 protein. CW2 (A) and Caco-2 cells (B) were treated with HUHS1015 (100  $\mu$ M) for 30 min in the absence and presence of 3-methyladenine (3-MA) (10 mM), followed by Western blotting. In the graphs, each column represents the mean ( $\pm$  SEM) signal intensity for PKM2 relative to the intensity for  $\beta$ -actin (n=4 independent experiments). *P* values, ANOVA followed by a Bonferroni correction



**Figure 4.** PKM2 knockdown. CW2 and Caco-2 cells were transfected with the NC siRNA or the PKM2 siRNA, and 48 h later Western blotting was carried out. In the graph, each column represents the mean ( $\pm$  SEM) signal intensity for PKM2 relative to the intensity for  $\beta$ -actin (n=4 independent experiments). *P* values, unpaired *t*-test.

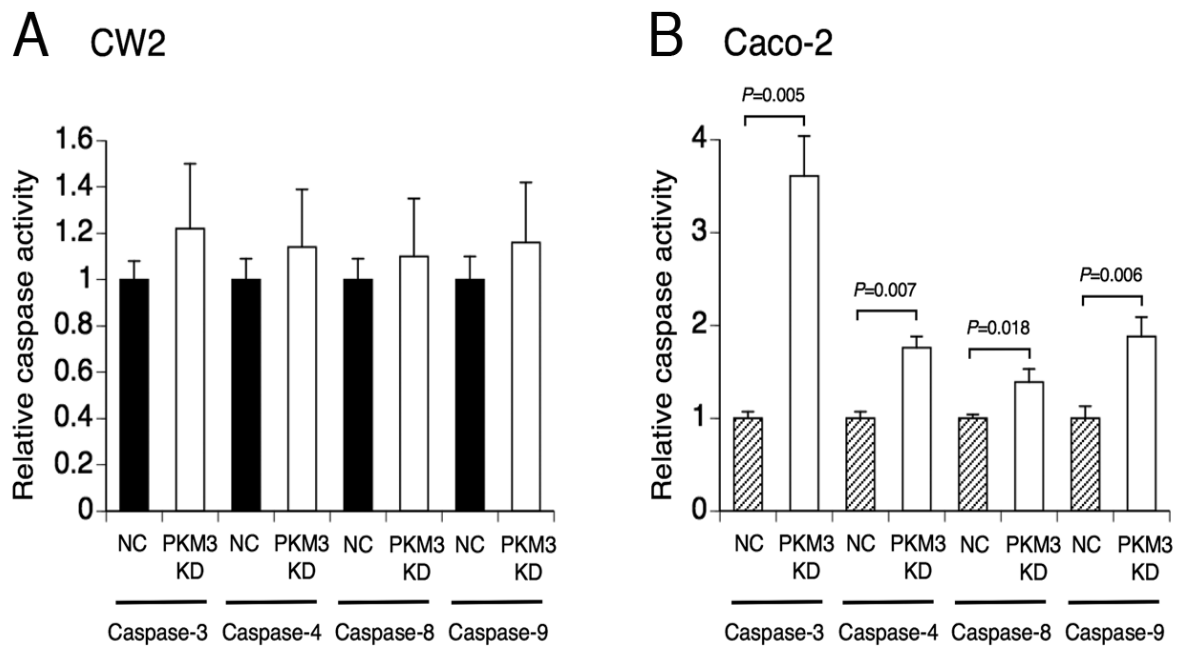


Figure 5. PKM2 deficiency activates caspase-3, -4, -8 and -9 in Caco-2 cells. CW2 (A) and Caco-2 cells (B) were transfected with the NC siRNA or the PKM2 siRNA, and 72 h later enzymatic caspase assay was performed. In the graphs, each column represents the mean ( $\pm$  SEM) ratio relative to the basal caspase activities in cells transfected with the NC siRNA (n=4 independent experiments). *P* values, unpaired *t*-test

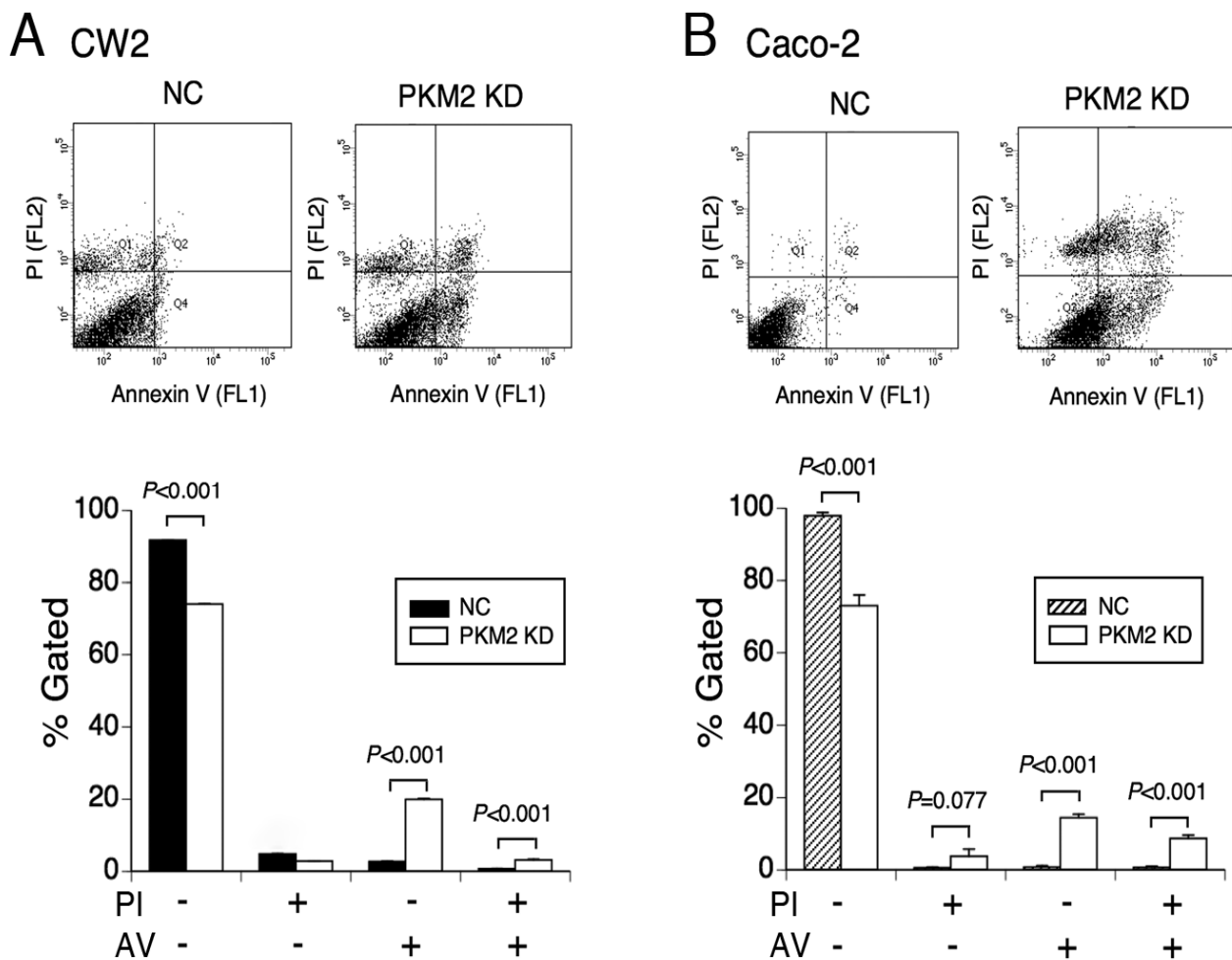


Figure 6. PKM2 deficiency induces necrosis/apoptosis. CW2 (A) and Caco-2 cells (B) were transfected with the NC siRNA or the PKM2 siRNA, and 72 h later flow cytometry using PI and AV was performed. In the graphs, each column represents the mean ( $\pm$  SEM) percentage of cells in four fractions against total cells (n=4 independent experiments). *P* values, unpaired *t*-test

the cell types. Notably, HUHS1015 markedly decreased PKM2 protein in CW2 and Caco-2 cells without affecting the PKM2 mRNA levels except for the decrease at 60-min treatment in CW2 cells, and the effect was cancelled by the autophagy inhibitor 3-MA. This implies that HUHS1015 decreases PKM2 protein mainly due to autophagic degradation. Autophagy is a process of degradation of macromolecules such as proteins and organelle in the cytoplasm, and impaired autophagy causes a variety of disorders including cancer and metabolic brain diseases (Pierzynowska *et al.*, 2018). In our earlier study, HUHS1015 also decreased XIAP due to autophagic degradation in CW2 cells (Tsuchiya *et al.*, 2015). This, taken together with the present results, raises the possibility that HUHS1015 has the potential to stimulate autophagy. It is presently unknown how HUHS1015 selects targets of autophagy and stimulates autophagy or whether HUHS1015 stimulates autophagy of other proteins except for PKM2 and XIAP. Pyruvate kinase catalyzes the formation of ATP from ADP, and the ATP generation is independent of oxygen supply, allowing survival of the organs under hypoxic conditions as seen in solid cancers (Vaupel and Harrison, 2004). Accumulating evidence has pointed to the role of PKM2 in the oncogenesis, progression, and prognosis of cancers (Hsu and Hung, 2018; Li *et al.*, 2018). PKM2 is upregulated in most cancer cells (Christofk *et al.*, 2008; Hamabe *et al.*, 2014; Steinberg *et al.*, 1999) and regulates cancer through diverse signaling pathways (Li *et al.*, 2014). PKM2 overexpression promotes colorectal cancer cell migration and cell adhesion by regulating STAT3-associated signaling (Yang *et al.*, 2014). PKM2, alternatively, promotes cell migration through pathways linked to phosphatidylinositol-3-kinase (PI3K)/Akt and Wnt/ $\beta$ -catenin signaling in colonic cancer cells (Yang *et al.*, 2015). PKM2, thus, could become a promising target for cancer therapy. Indeed, apigenin, an anticancer agent, restrains colonic cancer cell proliferation by blocking PKM2 (Shan *et al.*, 2017). LY294002, a PI3K inhibitor, exhibits an anticancer effect on gastric cancer by downregulating PKM2 (Lu *et al.*, 2018). Pantoprazole, a proton pump inhibitor, inhibits human gastric adenocarcinoma SGC-7901 cells by reducing expression of PKM2 (Shen *et al.*, 2016). Metformin suppresses gastric cancer by inhibiting hypoxia inducible factor 1 $\alpha$ /PKM2 signaling (Chen *et al.*, 2015). In the present study, PKM2 deficiency significantly activated caspase-3, -4, -8, and -9 in Caco-2 cells, although the caspase activities in CW2 cells were not affected. PKM2 deficiency, on the other hand, induced apoptosis as well as necrosis in CW2 and Caco-2 cells. Overall, these results indicate that HUHS1015-induced decrease of PKM2 protein could be a factor to induce cell death in CW2 and Caco-2 cells.

## Conclusion

The results of the present study demonstrate that HUHS1015 decreases PKM2 protein mainly due to autophagic degradation, causing cell death including necrosis and caspase-dependent and -independent apoptosis in CW2 and Caco-2 cells. This may represent further insight into the anticancer actions of HUHS1015.

## REFERENCES

Chen, G., Feng, W., Zhang, S. *et al.* 2015. Metformin inhibits gastric cancer via the inhibition of HIF1 $\alpha$ /PKM2 signaling. *Am. J. Cancer Res.*, 5:1423-1434.

- Christofk, H.R., Vander Heiden, M.G., Wu, N., *et al.* 2008. Pyruvate kinase M2 is a phosphotyrosine-binding protein. *Nature*, 452:181-186.
- Hamabe, A., Konno, M., Tanuma, N., *et al.* 2014. Role of pyruvate kinase M2 in transcriptional regulation leading to epithelial-mesenchymal transition. *Proc. Natl. Acad. Sci. USA*, 111:15526-15531.
- Hsu, M.C., Hung, W.C. 2018. Pyruvate kinase M2 fuels multiple aspects of cancer cells: from cellular metabolism, transcriptional regulation to extracellular signaling. *Mol. Cancer*, 17:35.
- Kaku, Y., Tsuchiya, A., Shimizu, T., *et al.* 2016. HUHS1015 suppresses colonic cancer growth by inducing necrosis and apoptosis in association with mitochondrial damage. *Anticancer Res.*, 36:39-48.
- Kanno, T., Tanaka, A., Shimizu, T., *et al.* 2013. 1-[2-(2-Methoxyphenylamino) ethylamino]-3-(naphthalene-1-yl)oxy) propan-2-ol as a potential anticancer drug. *Pharmacology*, 91:339-345.
- Li, Y.H., Li, X.F., Liu, J.T., *et al.* 2018. PKM2, a potential target for regulating cancer. *Gene*, 668:48-53.
- Li, Z., Yang, P., Li, Z. 2014. The multifaceted regulation and functions of PKM2 in tumor progression. *Biochim. Biophys. Acta*, 1846:285-296.
- Lu, J., Chen, M., Gao, S., *et al.* 2018. LY294002 inhibits the Warburg effect in gastric cancer cells by downregulating pyruvate kinase M2. *Oncol. Lett.*, 15:4358-4364.
- Nishizaki, T., Kanno, T., Tsuchiya, A., *et al.* 2014. 1-[2-(2-Methoxyphenylamino) ethylamino]-3-(naphthalene-1-yl)oxy) propan-2-ol may be a promising anticancer drug. *Molecules*, 19:21462-21472.
- Pierzynowska, K., Gaffke, L., Cyske, Z., *et al.* 2018. Autophagy stimulation as a promising approach in treatment of neurodegenerative diseases. *Metab. Brain Dis.*, 33:989-1008.
- Pietra, G., Mortarini, R., Parmiani, G., *et al.* 2001. Phases of apoptosis of melanoma cells, but not of normal melanocytes, differently affect maturation of myeloid dendritic cells. *Cancer Res.*, 61:8218-8226.
- Saitoh, M., Nagai, K., Nakagawa, K., *et al.* 2011. Adenosine induces apoptosis in the human gastric cancer cells via an intrinsic pathway relevant to activation of AMP-activated protein kinase. *Biochem. Pharmacol.*, 67:2005-2011.
- Shan, S., Shi, J., Yang, P., *et al.* 2017. Apigenin restrains colon cancer cell proliferation via targeted blocking of pyruvate kinase M2-dependent glycolysis. *J. Agric. Food Chem.*, 65:8136-8144.
- Shen, Y., Chen, M., Huang, S., *et al.* 2016. Pantoprazole inhibits human gastric adenocarcinoma SGC-7901 cells by downregulating the expression of pyruvate kinase M2. *Oncol. Lett.*, 11:717-722.
- Steinberg, P., Klingelhöffer, A., Schäfer, A., *et al.* 1999. Expression of pyruvate kinase M2 in preneoplastic hepatic foci of *N*-nitrosomorpholine-treated rats. *Virchows Arch.*, 434:213-220.
- Tsuchiya, A., Kaku, Y., Shimizu, T., *et al.* 2015. XIAP is a target for HUHS1015-induced caspase-3 activation in CW2 colonic cancer cells. *Int. J. Biol. Pharm. Res.*, 6:978-981.
- Vaupel, P., Harrison, L. 2004. Tumor hypoxia: causative factors, compensatory mechanisms, and cellular response. *Oncologist*, 9 Suppl 5:4-9.
- Yang, D., Yaguchi, T., Yamamoto, H., *et al.* 2007. Intracellularly transported adenosine induces apoptosis in HuH-7 human hepatoma cells by downregulating c-FLIP

- expression causing caspase-3/-8 activation. *Biochem. Pharmacol.*, 73:1665-1675.
- Yang, P., Li, Z., Fu, R., *et al.* 2014. Pyruvate kinase M2 facilitates colon cancer cell migration via the modulation of STAT3 signalling. *Cell Signal.*, 26:1853-1862.
- Yang, P., Li, Z., Wang, Y., *et al.* 2015. Secreted pyruvate kinase M2 facilitates cell migration via PI3K/Akt and Wnt/ $\beta$ -catenin pathway in colon cancer cells. *Biochem. Biophys. Res. Commun.*, 459:327-332.

\*\*\*\*\*